geosciences

MDPI

Article

Potential Instability of Gas Hydrates along the Chilean Margin Due to Ocean Warming

Giulia Alessandrini [1,*], Umberta Tinivella [2], Michela Giustiniani [2], Iván de la Cruz Vargas-Cordero [3] and Silvia Castellaro [1]

1 Dipartimento di Fisica e Astronomia, Sezione Geofisica, Università di Bologna, 40127 Bologna, Italy; silvia.castellaro@unibo.it
2 Istituto Nazionale di Oceanografia e di Geofisica Sperimentale (OGS), Borgo grotta gigante 42/c, 34010 Sgonico, Italy; utinivella@inogs.it (U.T.); mgiustiniani@inogs.it (M.G.)
3 Facultad de Ingeniería, Universidad Andres Bello, Quillota 980, Viña del Mar 2531015, Chile; ivan.vargas@unab.cl
* Correspondence: giulia.alessandrin11@unibo.it; Tel.: +39-085-2095169

Received: 22 March 2019; Accepted: 16 May 2019; Published: 21 May 2019

Abstract: In the last few years, interest in the offshore Chilean margin has increased rapidly due to the presence of gas hydrates. We have modelled the gas hydrate stability zone off Chilean shores (from 33° S to 46° S) using a steady state approach to evaluate the effects of climate change on gas hydrate stability. Present day conditions were modelled using published literature and compared with available measurements. Then, we simulated the effects of climate change on gas hydrate stability in 50 and 100 years on the basis of Intergovernmental Panel on Climate Change and National Aeronautics and Space Administration forecasts. An increase in temperature might cause the dissociation of gas hydrate that could strongly affect gas hydrate stability. Moreover, we found that the high seismicity of this area could have a strong effect on gas hydrate stability. Clearly, the Chilean margin should be considered as a natural laboratory for understanding the relationship between gas hydrate systems and complex natural phenomena, such as climate change, slope stability and earthquakes.

Keywords: gas hydrate; modelling; climate change; Chilean margin; slope stability; earthquake

1. Introduction

Many scientists worldwide have been working to better understand the onshore and offshore distribution of gas hydrate and its stability conditions. Natural gas hydrate is studied for a number of reasons, e.g., hydrate accumulations can store large amounts of natural gas, which could represent a potential energy resource (i.e., [1,2]).

Gas hydrates play an important role in the Chilean margin, mainly on account of critical issues concerning their potential dissociation. In fact, any variation in pressure and/or temperature conditions can lead to gas hydrate dissociation [3]. This may occur in the near future, as modelled by several previous studies (e.g., [4]), since the most recent assessment made by International Panel on Climate Change [5] confirmed that climate change may result in rising ocean temperatures and sea level. The release of huge quantities of natural gas in the water column could affect the marine ecosystem resulting in significant impact to benthic organisms [6]. Furthermore, methane is an important greenhouse gas, so after its release into the ocean, it could reach the atmosphere, resulting in positive feedback for global warming, as underlined by previous studies [7–9], although this is still the subject of debate among the scientific community (i.e., [10–13]). In fact, many factors prevent the methane from gas hydrate from reaching the atmosphere, such as methane release velocities and rates from the subsurface, and methane oxidation to carbon dioxide by microbial and chemical processes [14].

In recent years, the relationship between gas hydrate and submarine slides has been widely studied (e.g., [15]). Excess pore pressure has been identified as a key parameter in assessing slope instability [16]. Shear strain resistance significantly increases in hydrate-bearing sediments compared to hydrate-free sediments (e.g., [17]); during gas hydrate dissociation, released gas could increase the local pore fluid pressure in the sediment. This leads to a decrease of normal stress and, as a consequence, the formation of weak layers, in which less shear stress is needed to trigger failure (e.g., [18]). For this reason, the change in mechanical characteristics of marine sediments due to gas hydrate dissociation could lead to slope instability (e.g., [15]). Submarine slides would affect (i) gas hydrate stability itself, (ii) marine ecosystems, (iii) seafloor infrastructure and (iv) coastal areas, due to tsunamis that could be triggered [19].

The presence of gas hydrate in the Chilean margin has been confirmed by several geophysical cruises, in particular along the accretionary prism [20–22]. Gas hydrate has been detected in water depths up to 4 km with a depth range of 100–600 m below the seafloor (m b.s.f.) [13,23–28]. During ODP Leg 141, drill holes near the Chile Triple Junction sampled gas hydrates [29]. Mean volume concentrations of 18% and 1% have been observed for gas hydrate and free gas, respectively [20]. Recently, seismic data analysis confirmed the presence of gas hydrate and free gas, estimating concentration values in agreement with direct measurements [13,27,28,30,31]. In addition, studies off Valdivia estimated about 3.5% gas hydrate saturation in the pore space of marine sediments [21,30].

The study area is located in the southern segment of the central Peru-Chile margin (Figure 1) from 33° S to 46° S, covering about 1500 km from North to South. It includes the offshore regions from Valparaíso to Península de Taitao. In this area, the oceanic Nazca Plate subducts eastward, under the continental South American Plate, with an average convergence rate of about 8 cm/y [32–38].

The Juan Fernández and Chile ridges are the main bathymetric anomalies and represent the northern and southern boundaries for the study area, respectively [39]. The study area is characterized by a high sedimentation rate due to rapid erosion of the Andes and efficient fluvial transport, resulting in turbidite trench infill greater than 2 km [40].

Methane hydrate is stable in seafloor sediments at depths greater than 500 m below sea level (m b.s.l.), considering the equations of Sloan [3], as modelled by Tinivella et al. [18]. For the above considerations, this work aims to make a preliminary evaluation of the stability of gas hydrate and the possible effect of climate change on its stability by using a steady state approach along the Chilean margin.

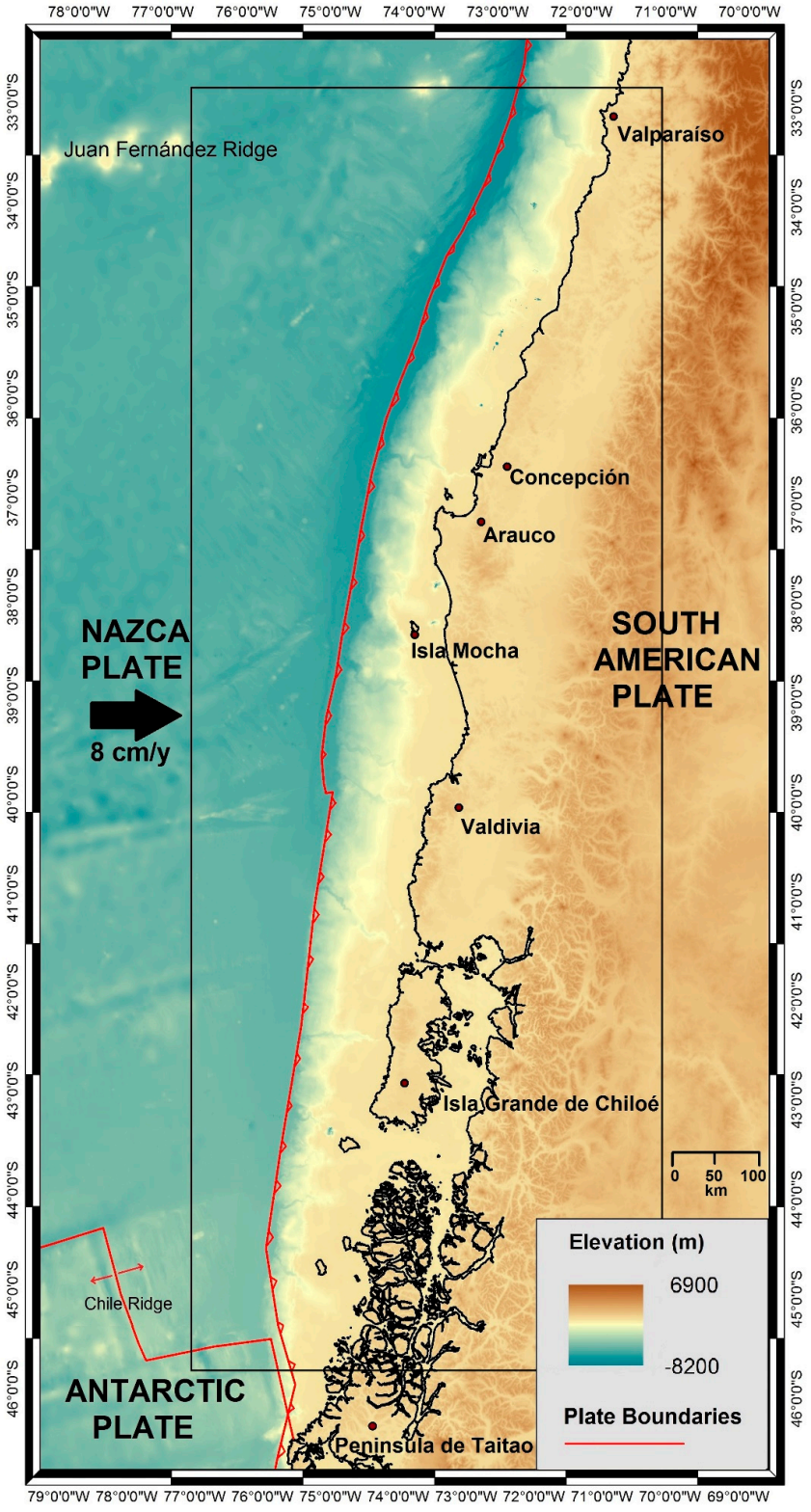

Figure 1. Topography and major tectonic elements of the study area. The black rectangle shows a sub-set of the study area selected for this work. The modelled area is the shelf-slope system, in which seafloor depths reach more than 500 m b.s.l.

2. Materials and Methods

2.1. Data Collection and Analysis

Gas hydrate stability on continental margins is a function of hydrostatic pressure, seafloor temperature, salinity, geothermal gradient and gas composition [3]. To model the Gas Hydrate Stability Zone (GHSZ) on the Chilean margin, the above-mentioned data have been gathered through bibliographic sources and available databases. Data analysis was performed using Geographic Information System (GIS) methods.

Bathymetry. In order to consider the hydrostatic pressure in our modelling, a bathymetric model (Figure 1) was downloaded from the GMRT website [41]. For this work, a WGS84 projection was chosen. The selected area from 33° S to 46° S and from 77° W to 71.5° W was imported and managed in GIS.

Seafloor temperature. Seafloor temperature data are available on the National Oceanographic Data Center website [42]. The selected data for the modelling area were interpolated in order to create a 500 × 500 m cell seafloor temperature grid (Figure 2A). A comparison between the bathymetric model and the seafloor temperature distribution suggests that seafloor topography strongly affects water mass temperatures as expected. In fact, colder waters (1 °C) fill deeper basins, while eastward, close to the Chilean shoreline, water temperatures are higher (13 °C).

Water column salinity. Water column salinity data were downloaded from the National Oceanographic Data Center website [42]. The selected data for the modelling area were imported in GIS and interpolated in a 500 × 500 m cell salinity grid. Figure 2B shows a water column salinity that varies between 33 and 34.

Geothermal gradient. Geothermal gradient data have been derived from the heat flow/thermal conductivity ratio. First, the heat flow and the thermal conductivity grids were built. To do this, heat flow data have been gathered, merged together and interpolated in a 500 × 500 m cell grid. They come from direct and indirect measurements. Heat flow data were collected during ODP Legs 141 and 202 [29,34,43]. The indirect data have been obtained from seismic data acquired along the Chilean margin, using the heat flow calculation method of Cande et al. [23] and reported in Villar-Muñoz et al. [44]. They show a progressive regional increase of the heat flow values from North to South: from about 24 mW/m^2, off Valparaíso, to 250 mW/m^2, close to the Chile Triple Junction.

Conductivity data come from a regional estimate, based on data collected during ODP Legs 141 and 202 [29,34,43,44]. Based on the average measured values, in the northern region the thermal conductivity was assumed equal to 0.85 W mK^{-1} [34,44], whereas in the southern area it decreases to 1.25 W mK^{-1} [29,43]. These data were interpolated through a linear regression algorithm in order to build a thermal conductivity grid. Combining the heat flow and the thermal conductivity grids, it was possible to calculate the geothermal gradient grid. Nevertheless, it was not possible to display the geothermal gradient in a map, because the number of data available for the interpolation was too low if compared to the previous two grids. The average geothermal gradient is around 49°C/km, which is consistent with previous observations [43].

Gas composition. Based on log and downhole temperature measurements carried out during ODP Legs 141 and 202 [43,45], the composition of gas hydrate in these sites is mainly methane. Unfortunately, no other direct measurements are available regarding the gas composition along the entire margin. So, we considered a pure methane hydrate that is more sensitive to climate change, as demonstrated by several authors (e.g., [46]).

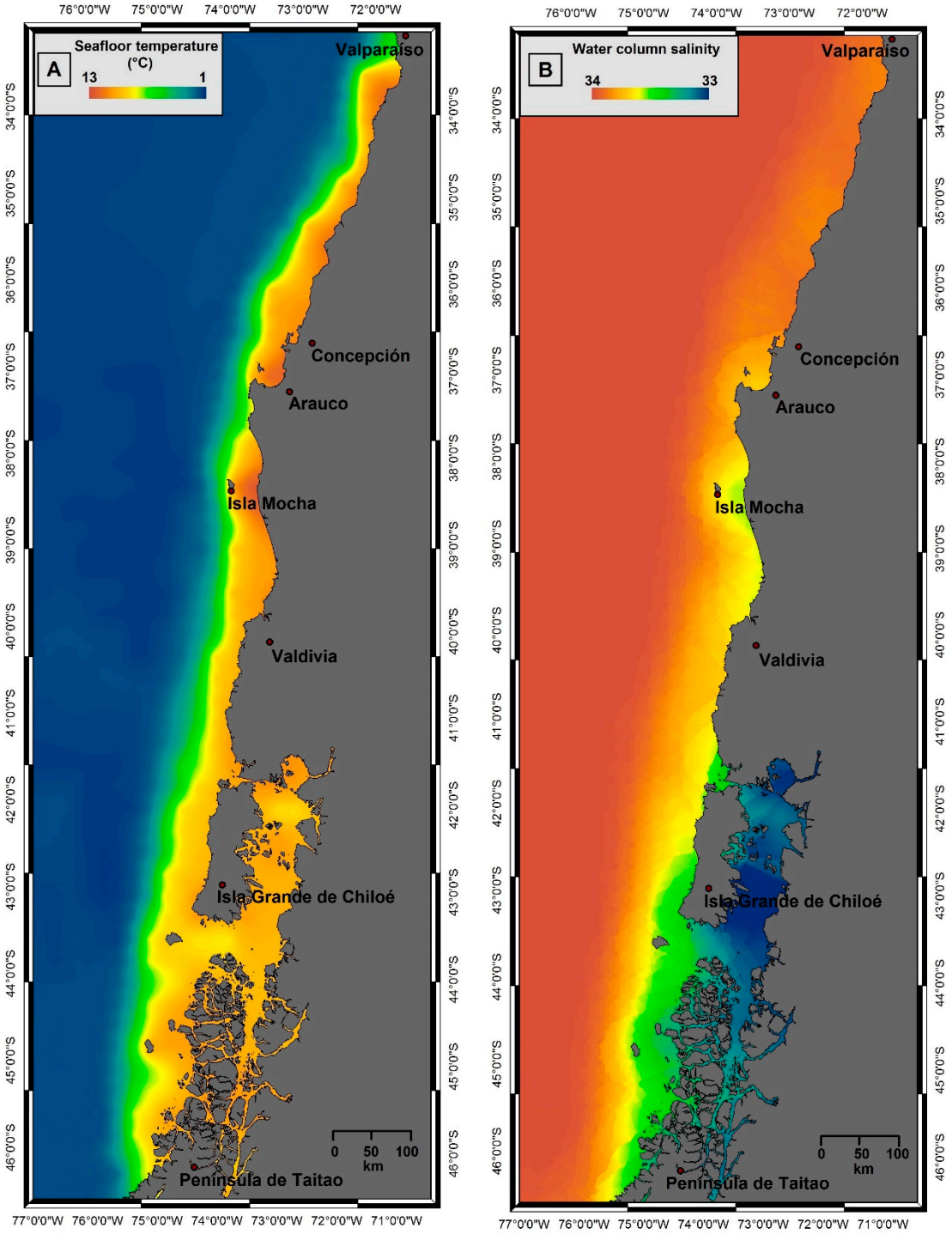

Figure 2. (**A**) Seafloor temperature grid. (**B**) Water column salinity grid.

2.2. Modelling

We adopted a steady state approach to model the base of the GHSZ assuming that: (a) a seabed temperature perturbation drives heat and has sufficient time to diffuse through the entire GHSZ; (b) during that time gas hydrate does not form or dissociate within the GHSZ; and (c) there is no latent heat. First, we simulated the present-day conditions in order to evaluate the zones where gas hydrate stability is verified (hereafter called "Scenario *S0*") using the above described data. The base of the GHSZ was defined as the intersection between the gas hydrate stability curve and the geothermal

curve (i.e., [18,47]). The modelling considers Sloan equations [3], concerning gas hydrates equilibrium phases, and Dickens & Quinby-Hunt formula [48], which considers different salinity values. Applying this approach, the depth of the base of GHSZ (z_{GHSZ}) was calculated by solving the following equation:

$$\{7.054 \times 10^{-3} - 2.83 \times 10^{-4} \times [\log \cdot \varrho_w + \log (z_w + z_{GHSZ})]\} \times (T_0 + 273.15 + 1 \times 10^{-3}\ GG\ z_{GHSZ}) = 1,$$

where z_w is the water depth (m), T_0 is the seafloor temperature (°C), GG is the geothermal gradient (°C/km) and ϱ_w is the water density (i.e., [46]). The input data for this calculation were the above described manipulated dataset, described in Section 2.1.

Considering the Intergovernmental Panel on Climate Change (IPCC) [5] and National Aeronautics and Space Administration (NASA) [49] forecasts for future global warming, we simulated the effects of climate change on the GHSZ. More precisely, we considered different seafloor temperature increases (ΔT) and different sea level rises (Δs.l.), for 50- and 100-year-long terms. Based on the above cited forecasts, the following scenarios were modelled:

Scenarios in 50 years:

- *S1*: $\Delta T = 2$ °C,
- *S2*: Δs.l. = 1.6 m,
- *S3*: $\Delta T = 2$ °C and Δs.l. = 1.6 m.

Scenarios in 100 years:

- *S4*: $\Delta T = 4$ °C,
- *S5*: Δs.l. = 3.2 m,
- *S6*: $\Delta T = 4$ °C and Δs.l. = 3.2 m.

3. Results

The depth of the base of GHSZ for the Scenario *S0* is mapped in Figure 3. With sufficient methane, gas hydrate could form from the seafloor down to 580 m b.s.f. along the lower slope, in which bathymetric depths are as great as 6 km. The results of our modelling are in agreement with geophysical data, as reported in Coffin et al. [50]. Travelling to the east, along the upper slope, the base of the GHSZ becomes shallower until it intersects the seafloor at about 500 m b.s.l. (Figure 3). The area of this intersection is the most sensitive to seafloor temperature variations due to its smaller thickness, as observed by Marín-Moreno et al. [51]. To assess the error in modelling, we consider the error estimated by seismic velocity model perturbation to be 5% because the geothermal gradients were obtained from seismic data [22], and the error in bathymetric data as 1.5% in agreement with Tinivella et al. [18].

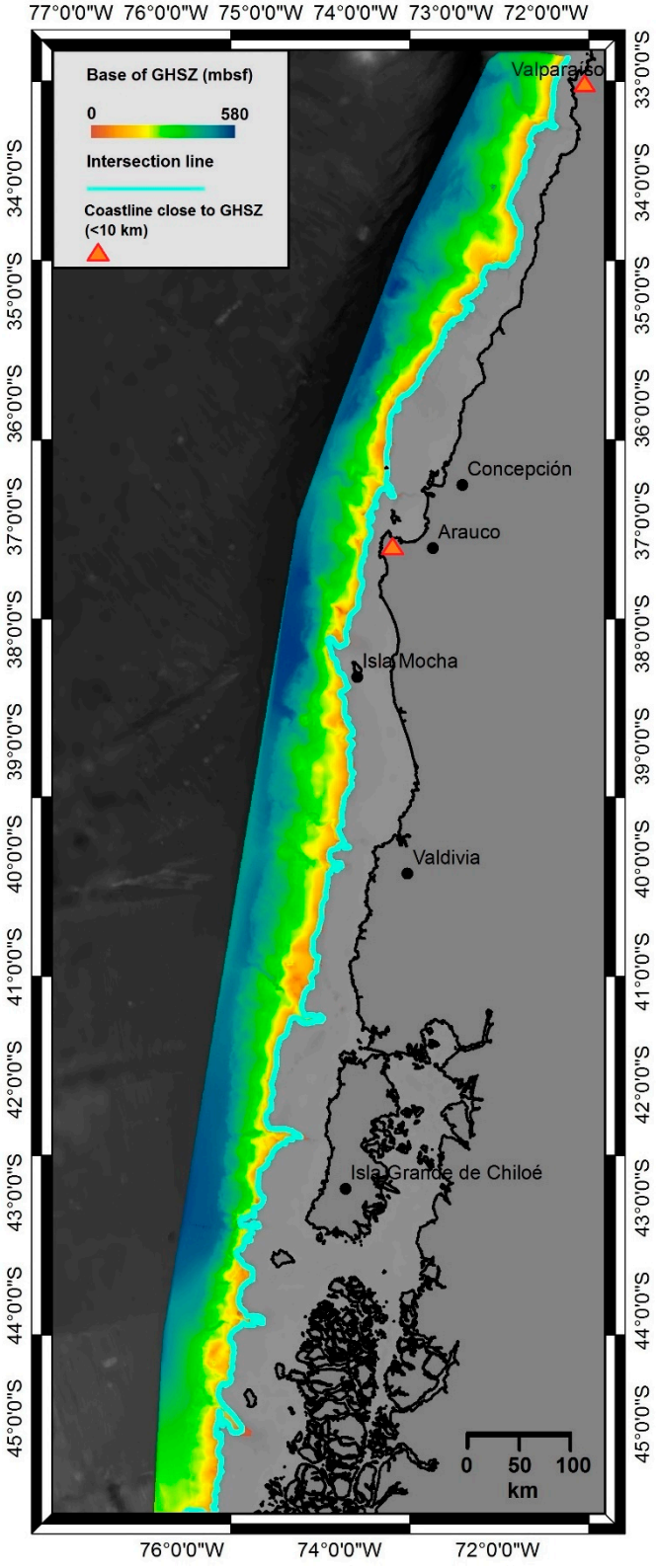

Figure 3. Depth of the base of the GHSZ below the seafloor for Scenario *S0* (present-day conditions). The base of the GHSZ is deeper for cool colors (lower slope) and shallower for warm colors (upper slope-shelf). The light-blue line marks the intersection between the base of the GHSZ and the seafloor. The red triangles highlight coastal locations very close to the intersection.

Figures 4 and 5 show the results of our modelling for present and future scenarios. For each of them, it was possible to model and calculate the thickness of the GHSZ. For future scenarios, these values were compared to the present Scenario *S0*, in order to observe possible variations in terms of thickness. Figure 4 shows for each scenario the average water depth at which the base of the GHSZ intersects the seafloor, considering the estimated error. Figure 5 reports for each scenario the average thickness of GHSZ sampled every 100 m.

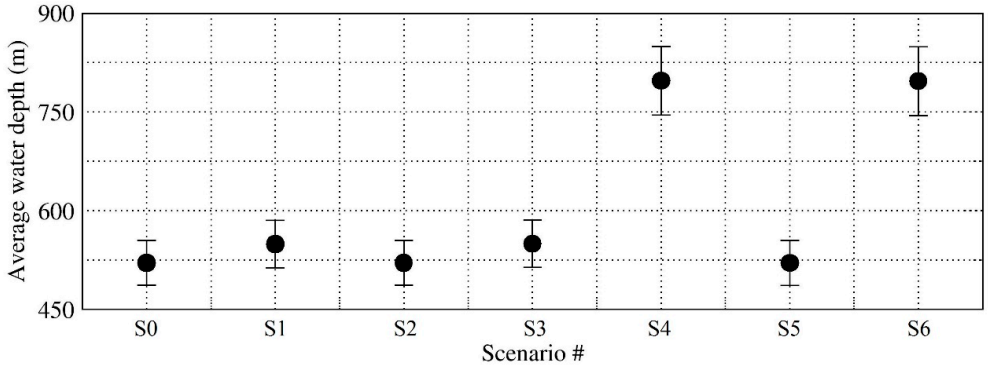

Figure 4. Average water depth at which the base of the GHSZ intersects the seafloor, considering the estimated error.

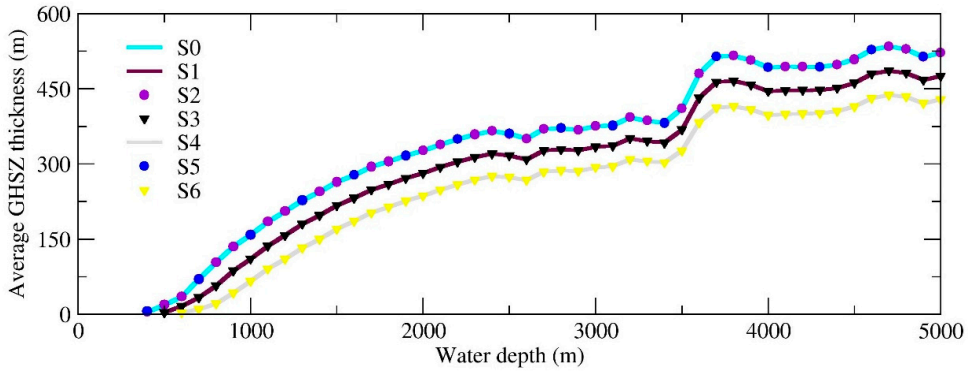

Figure 5. Average thickness of GHSZ. In every scenario, the thickness increases from the shelf-upper slope to the lower slope.

4. Discussion

The modelling results show that the predicted changes in climate could affect gas hydrate stability in the Chilean margin. Due to the small modelled increase in sea level, the *S2* and *S5* scenarios show a negligible variation compared to *S0* (Figures 4 and 5). In addition, *S3* and *S6* show a negligible variation compared to *S1* and *S4*, respectively (Figures 4 and 5). Considering different temperature increases (*S1* and *S4*), the modelled GHSZ would be reduced in terms of thickness and the average water depth for stability conditions would be greater with respect to *S0*.

Table 1 reports the two future scenarios in which seafloor temperature increase was considered. Global warming initially affects the stability of gas hydrate located in the proximity of the intersection between the base of the GHSZ and the seafloor [51] in the shallow upper slope-shelf. It is worth highlighting that the increase of 2 °C in seafloor temperature (*S1*) is almost the same observed for *S3*, where 2 °C temperature increase is combined with a pressure increase due to 1.6 m sea level rise. In both cases, in fact, there would be total gas hydrate dissociation in about 3% of the area in which gas hydrates are stable at present (*S0*). The effects of global warming in 100 years would be similar but amplified. In fact, in both *S4* and *S6*, there could be a potential release of the gas in 6.5% of the area in which the gas hydrate is stable at present (*S0*). It is possible to identify two zones (offshore Arauco

Peninsula and Valparaíso) in which the intersection between the seafloor and the base of the GHSZ is nearby to the shoreline (close to 10 km; Figure 3). Considering this, the potential dissociation could have dangerous consequences for coastal cities and infrastructure because of possible slope instability.

Table 1. Amount of gas released by thermal dissociation of gas hydrate, considering a porosity of 40% and a mean hydrate saturation of 3% according to the minimum value proposed by [21,30].

Scenario	Gas Hydrate Dissociation Area	Total Volume	Pore Volume	Hydrate Volume	Gas Volume
***S1* (ΔT = 2 °C)**	3%	113 km^3	45 km^3	1.36 km^3	222 km^3
***S4* (ΔT = 4 °C)**	6.5%	482 km^3	193 km^3	5.79 km^3	950 km^3

At standard pressure and temperature conditions, about 164 m^3 of methane are contained in 1 m^3 of gas hydrate. So, according to our modelling, in the next 50 years, there could be a potential release of 222 km^3 of methane from hydrate dissociation for *S1* (Table 1). On the other hand, in the next 100 years there could be a potential emission of 950 km^3 of methane for *S4* (Table 1). However, steady state models, which represent the hydrate system at the equilibrium after a warming or cooling period, could overestimate emission of gas from hydrate. In fact, the non-inclusion of thermodynamics processes, like self-preservation of gas hydrate [52] and the time of propagation of heat through the entire thickness of sediments could lead to a too rapid disappearance of the GHSZ during warming events [53].

To show clearly the possible effects of global warming, Figure 6 reports the intersections between the seafloor and the base of the GHSZ for all scenarios, focusing on an area characterized by strong slope gradients (35°–38° S). Note that the lines related to *S0*, *S2* and *S5* roughly overlap as well as *S1–S3* and *S4–S6*, as already discussed; arrows represent the dip direction and their size is directly proportional to the slope degree.

In the selected sector reported in Figure 6, due to the tectonic-sedimentary configuration, the area is characterized by high angle slopes and, for this reason, unstable in the long term. In fact, high basal frictions in convergent margins give rise to oversteepening and, therefore, more unstable accretionary prisms [40]. If combined with local high sedimentation rate, these two factors could create some critical areas with high risk for slope failure. Several authors have suggested that in the area reported in Figure 6 the above conditions are verified and several slope failures are documented (e.g., [54–56]). In fact, more than 60 submarine slopes were mapped in the area between 35° S to 38° S. Among these, Valdes Slide, Reloca Slide and the Northern, Central and Southern Embayments are the most noticeable lower-continental slides because of their size and volume [54–57]. In addition, most of the slope failures mapped in this area are related to submarine canyons, mainly on the upper-continental slope [56]. These critically-stable continental slopes are more susceptible areas to slide risk if gas hydrate dissociation is considered [16]. It is important to remind ourselves that the combination of critically-stable slopes and the proximity of the intersections to the coast contributes to define the potential instability of this area.

In Figure 6, average slope values along the modelled intersections are about 10°, up to 20° at submarine canyons (e.g., Bío Bío Canyon). It is clear that the effect of the temperature increase modelled in *S4* and *S6* could be potentially more critical in the proximity of the high degree slopes, located not far from the coast. Also, active and fossil fluid venting, such as authigenic carbonates, along the upper slope between 36.5° and 36.8° S seems to contribute to the potential weakening of sediment cohesion and help trigger submarine landslides [58]. Moreover, the critical submarine slope issue should be linked to the high seismicity characterizing the Chilean margin. In fact, areas characterized by high basal friction coefficients and steep slopes (Figure 6) could be particularly sensitive in case of an earthquake, promoting slides with potential gas hydrate dissociation. In particular, the selected area has been affected by the strongest earthquakes ever recorded, such as the Mw 9.5 (1960) and the Mw 8.8 (2010) events, both with very shallow hypocenters [59] (Figure 6).

Recent studies show that slope stability in active margins is higher due to seismic strengthening, hence suggesting an inverse relationship between seismicity and submarine landslides [60–62]. Despite that, different authors [61,63] show that high sedimentation rates in continental slopes seem to be able to counteract seismic strengthening, which is thought to be particularly high in this sector, as mentioned before.

Finally, it is worth mentioning that, as already remarked by several authors (e.g., [19]), an earthquake could trigger gas hydrate dissociation. So, better understanding of the link between gas hydrate, slope stability and earthquakes is required.

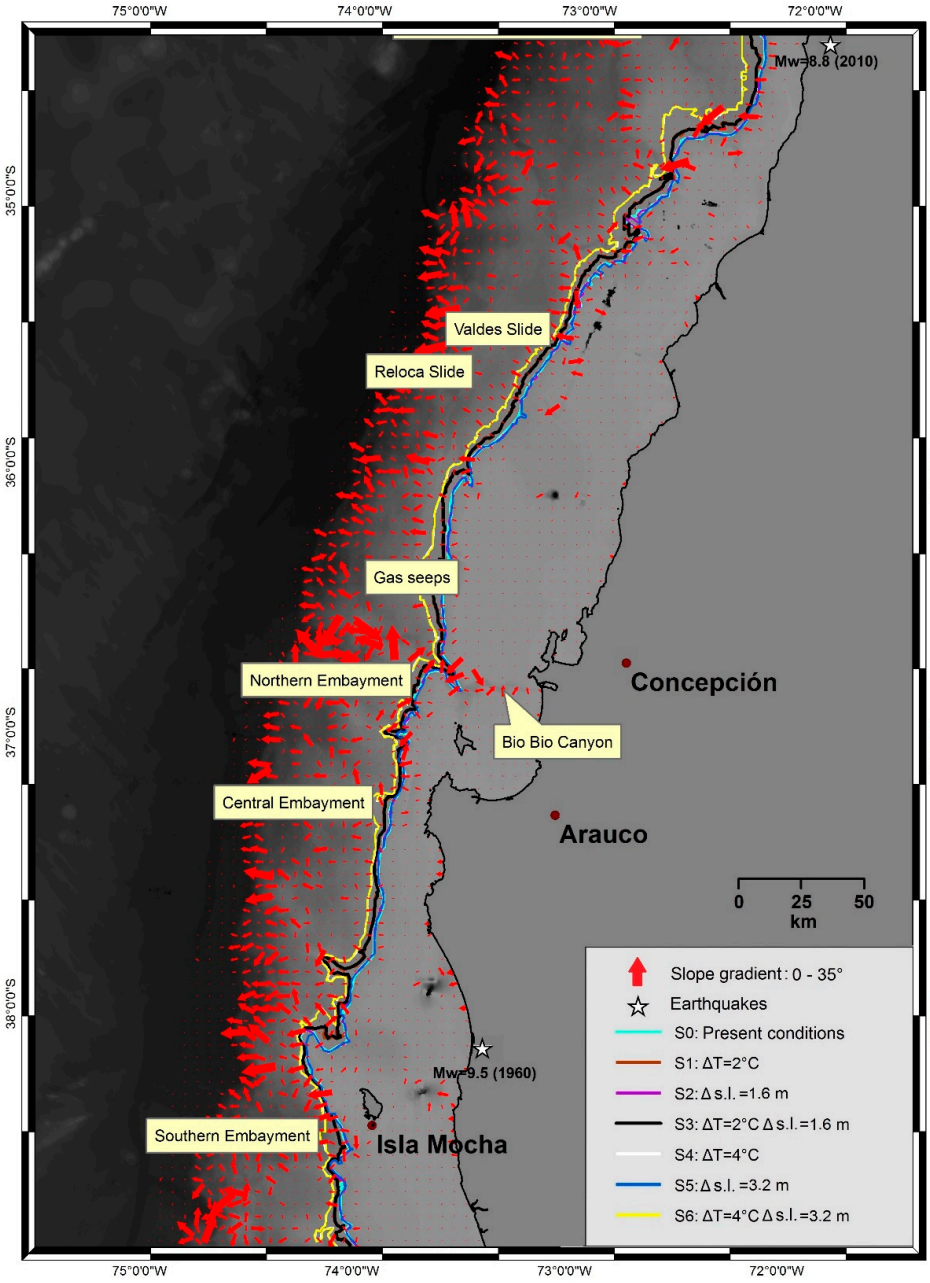

Figure 6. Study area between 35° S–38° S. The solid colored lines represent the intersections between the base of the GHSZ and the seafloor for each scenario. Here, the intersections are related to the slope gradient, marked by red arrows; the main slope failures are mapped, and major recent earthquakes are marked by stars.

5. Conclusions

We modelled the GHSZ using steady state modelling to verify where the gas hydrate could be stable along the Chilean margin and to evaluate in first approximation the possible effects of climate change on gas hydrate stability. Based on the model results, it was possible to estimate the thickness of marine sediments in which the conditions for the formation of gas hydrate are met.

Under present-day conditions (*S0)*, depending on methane availability, gas hydrates can form down to 580 m b.s.f., along the lower slope, as confirmed by Coffin et al. [50]. These authors integrated data from seismic surveys, geochemical analysis of porewater samples from piston cores and heat flow probing.

Considering the IPCC [5] and NASA [49] forecasts for the future global warming over the next 50 and 100 years, we simulated the impact of climate change on the GHSZ, for the first time ever for the Chilean margin. The modelled future scenarios, considering an increase in temperature (*S1*, *S3*, *S4*, *S6*), would indicate total gas hydrate dissociation along the upper slope. This suggests that, despite higher pressure due to sea level rise, the effect of the seafloor temperature increase on gas hydrate stability is significant. Sea level rise seems to be insufficient to counteract the effect of temperature increase, which is primarily responsible for GHSZ thinning [64].

The potential methane release due to gas hydrate dissociation could cause slope instability. Due to the tectonic-sedimentary configuration, the 35° S–38° S sector has been identified as potentially critical for the long term. As a consequence, coastal cities could be seriously damaged if tsunamis were triggered due to gas hydrate dissociation. Furthermore, the high seismicity of this area could significantly affect slope failure and consequently gas hydrate stability. An integrated approach is needed to understand the link between these processes.

In conclusion, our scenarios suggested that climate change could affect hydrate stability in long term. For this reason, transient modelling is necessary to understand how the hydrate dissociation could happen, since it shows how the hydrate system changes during the warming or cooling period until the equilibrium state. Moreover, an integration with geophysical data, in particular seismic data, could contribute to calibrate future models and to make appropriate assumptions on the initial gas hydrate distribution and saturation, which are inhomogeneous from down-slope to up-slope [53,65]. Furthermore, our steady state modelling demonstrates that more effort should be devoted to gaining a better understanding of the relationship between the gas hydrate system and complex natural phenomena, such as climate change, slope stability and earthquakes.

Author Contributions: Conceptualization and methodology, G.A., U.T., M.G. and I.V.-C.; writing—original draft preparation, G.A.; writing—review and editing, G.A., U.T., M.G., I.V.-C. and S.C.; supervision, U.T., M.G., I.V.-C. and S.C.

Funding: This research was partially supported by the Italian Ministry of Education, Universities and Research (Decreto MIUR No. 631 dd. 8 August 2016) under the extraordinary contribution for Italian participation in activities related to the international infrastructure PRACE—The Partnership for Advanced Computing in Europe (www.prace-ri.eu).

Acknowledgments: We want to thank the COST-MIGRATE Action (reference code ES1405-050317-082155). We would like to thank the anonymous reviewers for valuable comments.

Conflicts of Interest: The authors declare no conflict of interest.

References

1. Makogon, Y.F. *Hydrate of Hydrocarbons*; PennWell Publishing Co.: Tulsa, Oklahoma, 1997.
2. Moridis, G.J.; Collett, T.S.; Boswell, R.; Kurihara, M.; Reagan, M.T.; Koh, C.; Sloan, E.D. Toward production from gas hydrates: Current status, assessment of resources, and simulation-based evaluation of technology and potential. *SPE Reserv. Eval. Eng.* **2009**, *12*, 745–771. [CrossRef]
3. Sloan, E.D., Jr. *Clathrate Hydrates of Natural Gases*, 2nd ed.; Revised and Expanded; Marcel Dekker, Inc.: New York, NY, USA, 1998; p. 705.

4. Marín-Moreno, H.; Giustiniani, M.; Tinivella, U. The potential response of the hydrate reservoir in the South Shetland Margin, Antarctic Peninsula, to ocean warming over the 21st century. *Polar Res.* **2015**, *34*, 27443. [CrossRef]
5. IPCC. Contribution of Working Groups I, II and III to the Fifth Assessment Report of the Intergovernmental Panel on Climate Change. In *Climate Change 2014: Synthesis Report*; Pachauri, R.K., Meyer, L.A., Eds.; IPCC: Geneva, Switzerland, 2014; 151p.
6. Wallman, K.; MIGRATE Consortium. Marine Gas Hydrate—An Indigenous Resource of Natural Gas for Europe (MIGRATE). 2015; Available online: https://www.migrate-cost.eu/ (accessed on 29 April 2019).
7. MacDonald, I.; Joye, S. Lair of the "Ice Worm". *Quarterdeck* **1997**, *5*, 5–7.
8. Kvenvolden, K.A. Methane hydrate in the global organic carbon cycle. *Terra Nova* **2002**, *14*, 302–306. [CrossRef]
9. Kennett, J.P.; Cannariato, K.G.; Hendy, I.L.; Behl, R.J. *Role of Methane Hydrates in Late Quaternary Climatic Change: The Clathrate Gun Hypothesis*; AGU: Washington, DC, USA, 2003; Volume 54, 216p.
10. Dickens, G.R. Modeling the global carbon cycle with a gas hydrate capacitor: Significance for the latest Paleocene thermal maximum. In *Natural Gas Hydrates: Occurrence, Distribution, and Detection*; Paull, C.K., Dillon, W.P., Eds.; Geophysical Monograph Series; American Geophysical Union: Washington, DC, USA, 2001; Volume 124, pp. 19–40.
11. Xu, W.; Lowell, R.P.; Peltzer, E.T. Effect of seafloor temperature and pressure variations on methane flux from a gas hydrate layer: Comparison between current and late Paleocene climate conditions. *J. Geophys. Res. Solid Earth* **2001**, *106*, 26413–26423. [CrossRef]
12. Milkov, A.V. Global estimates of hydrate-bound gas in marine sediments: How much is really out there? *Earth-Sci. Rev.* **2004**, *66*, 183–197. [CrossRef]
13. Vargas-Cordero, I.; Tinivella, U.; Villar-Muñoz, L.; Bento, J. High Gas Hydrate and Free Gas Concentrations: An Explanation for Seeps Offshore South Mocha Island. *Energies* **2018**, *11*, 3062. [CrossRef]
14. Kvenvolden, K.A. Potential effects of gas hydrate on human welfare. *Proc. Natl. Acad. Sci. USA* **1999**, *96*, 3420–3426. [CrossRef]
15. Sultan, N.; Cochonat, P.; Foucher, J.P.; Mienert, J. Effect of gas hydrates melting on seafloor slope instability. *Mar. Geol.* **2004**, *213*, 379–401. [CrossRef]
16. Sultan, N.; Cochonat, P.; Canals, M.; Cattaneo, A.; Dennielou, B.; Haflidason, H.; Laberg, J.S.; Long, D.; Mienert, J.; Trincardi, F.; et al. Triggering mechanisms of slope instability processes and sediment failures on continental margins: A geotechnical approach. *Mar. Geol.* **2004**, *213*, 291–321. [CrossRef]
17. Tinivella, U. The seismic response to over-pressure versus gas hydrate and free gas concentration. *J. Seism. Explor.* **2002**, *11*, 283–305.
18. Tinivella, U.; Giustiniani, M.; Accettella, D. 2011. BSR versus climate change and slides. *J. Geol. Res.* **2011**, *2011*, 390547.
19. Boobalan, A.J.; Ramanujam, N. Triggering mechanism of gas hydrate dissociation and subsequent sub marine landslide and ocean wide Tsunami after Great Sumatra—Andaman 2004 earthquake. *Arch. Appl. Sci. Res.* **2013**, *5*, 105–110.
20. Bangs, N.L.; Sawyer, D.S.; Golovchenko, X. Free gas at the base of the gas hydrate zone in the vicinity of the Chile triple junction. *Geology* **1993**, *21*, 905–908. [CrossRef]
21. Rodrigo, C.; González-Fernández, A.; Vera, E. Variability of the bottom-simulating reflector (BSR) and its association with tectonic structures in the Chilean margin between Arauco Gulf (37° S) and Valdivia (40° S). *Mar. Geophys. Res.* **2009**, *30*, 1–19. [CrossRef]
22. Vargas-Cordero, I.; Tinivella, U.; Accaino, F.; Loreto, M.F.; Fanucci, F.; Reichert, C. Analyses of bottom simulating reflections offshore Arauco and Coyhaique (Chile). *Geo-Mar. Lett.* **2010**, *30*, 271–281. [CrossRef]
23. Cande, S.C.; Leslie, R.B.; Parra, J.C.; Hobart, M. Interaction between the Chile Ridge and Chile Trench: Geophysical and geothermal evidence. *J. Geophys. Res: Solid Earth* **1987**, *92*, 495–520. [CrossRef]
24. Froelich, P.N.; Kvenvolden, K.A.; Torres, M.E.; Waseda, A.; Didyk, B.M.; Lorenson, T.D. Geochemical evidence for gas hydrate in sediment near the Chile Triple Junction. *Proc. ODP Sci. Results* **1995**, *141*, 279–287.
25. Sloan, E.D., Jr.; Koh, C. *Clathrate Hydrates of Natural Gases*, 3rd ed.; CRC Press: Boca Raton, FL, USA, 2007; p. 752.

26. Vargas-Cordero, I.; Tinivella, U.; Accaino, F.; Fanucci, F.; Loreto, M.F.; Lascano, M.E.; Reichert, C. Basal and frontal accretion processes versus BSR characteristics along the Chilean margin. *J. Geol. Res.* **2011**, *2011*, 846101. [CrossRef]
27. Vargas-Cordero, I.; Tinivella, U.; Villar-Muñoz, L.; Giustiniani, M. Gas hydrate and free gas estimation from seismic analysis offshore Chiloé island (Chile). *Andean Geol.* **2016**, *43*, 263–274. [CrossRef]
28. Vargas-Cordero, I.; Tinivella, U.; Villar-Muñoz, L. Gas Hydrate and Free Gas Concentrations in Two Sites inside the Chilean Margin (Itata and Valdivia Offshores). *Energies* **2017**, *10*, 2154.
29. Grevemeyer, I.; Villinger, H. Gas hydrate stability and the assessment of heat flow through continental margins. *Geophys. J. Int.* **2001**, *145*, 647–660. [CrossRef]
30. Vargas-Cordero, I.; Tinivella, U.; Accaino, F.; Loreto, M.F.; Fanucci, F. Thermal state and concentration of gas hydrate and free gas of Coyhaique, Chilean Margin (44 30′ S). *Mar. Pet. Geol.* **2010**, *27*, 1148–1156. [CrossRef]
31. Villar-Muñoz, L.; Bento, J.P.; Klaeschen, D.; Tinivella, U.; Vargas-Cordero, I.; Behrmann, J.H. A first estimation of gas hydrates offshore Patagonia (Chile). *Mar. Pet. Geol.* **2018**, *96*, 232–239. [CrossRef]
32. Bangs, N.L.; Cande, S.C. Episodic development of a convergent margin inferred from structures and processes along the southern Chile margin. *Tectonics* **1997**, *16*, 489–503. [CrossRef]
33. Ramos, V. Plate tectonic setting of the Andean Cordillera. *Episodes* **1999**, *22*, 183–190.
34. Grevemeyer, I.; Diaz-Naveas, J.L.; Ranero, C.R.; Villinger, H.W. Heat flow over the descending Nazca plate in central Chile, 32 S to 41 S: Observations from ODP Leg 202 and the occurrence of natural gas hydrates. *Earth Planet. Sci. Lett.* **2003**, *213*, 285–298. [CrossRef]
35. Melnick, D. Neogene Seismotectonics of the South-Central Chile Margin: Subduction-Related Processes over Various Temporal and Spatial Scales. Ph.D. Thesis, Universität Potsdam, Potsdam, Germany, 2007.
36. Cembrano, J.; Lara, L. The link between volcanism and tectonics in the southern volcanic zone of the Chilean Andes: A review. *Tectonophysics* **2009**, *471*, 96–113. [CrossRef]
37. Vargas-Cordero, I. Gas Hydrate Occurrence and Morpho-Structures along Chilean Margin. Ph.D. Dissertation, Fisiche e Naturali, Università di Trieste, Trieste, Italy, 2009.
38. Manea, V.C.; Pérez-Gussinyé, M.; Manea, M. Chilean flat slab subduction controlled by overriding plate thickness and trench rollback. *Geology* **2012**, *40*, 35–38. [CrossRef]
39. Melnick, D.; Echtler, H.P. Inversion of forearc basins in south-central Chile caused by rapid glacial age trench fill. *Geology* **2006**, *34*, 709–712. [CrossRef]
40. Maksymowicz, A. The geometry of the Chilean continental wedge: Tectonic segmentation of subduction processes off Chile. *Tectonophysics* **2015**, *659*, 183–196. [CrossRef]
41. GMRTMapTool. Available online: https://www.gmrt.org/GMRTMapTool/ (accessed on 29 April 2019).
42. National Oceanographic Data Center (NODC). Available online: https://www.nodc.noaa.gov/OC5/woa13/woa13data.html (accessed on 29 April 2019).
43. Bangs, N.L.; Brown, K.M. Regional heat flow in the vicinity of the Chile Triple Junction constrained by the depth of the bottom simulating reflection. *Proc. ODP Sci. Results* **1995**, *141*, 253–259.
44. Villar-Muñoz, L.; Behrmann, J.H.; Diaz-Naveas, J.; Klaeschen, D.; Karstens, J. Heat flow in the southern Chile forearc controlled by large-scale tectonic processes. *Geo-Mar. Lett.* **2014**, *34*, 185–198.
45. Mix, A.C.; Tiedemann, R.; Blum, P. *Shipboard Scientific Party Proceedings of the ODP*; Initial Reports; Ocean Drilling Program: College Station, TX, USA, 2003; pp. 1–145.
46. Tinivella, U.; Giustiniani, M. Variations in BSR depth due to gas hydrate stability versus pore pressure. *Glob. Planet. Chang.* **2013**, *100*, 119–128. [CrossRef]
47. Khan, M.J.; Ali, M. A Review of Research on Gas Hydrates in Makran. *Bahria Univ. Res. J. Earth Sci.* **2016**, *1*, 28–35.
48. Dickens, G.R.; Quinby-Hunt, M.S. Methane hydrate stability in pore water: A simple theoretical approach for geophysical applications. *J. Geophys. Res.* **1997**, *102*, 773–783. [CrossRef]
49. NASA Global Climate Change. Available online: https://climate.nasa.gov/scientific-consensus/ (accessed on 29 April 2019).
50. Coffin, R.; Pohlman, J.; Gardner, J.; Downer, R.; Wood, W.; Hamdan, L.; Walker, S.; Plummer, R.; Gettrust, J.; Diaz, J. Methane hydrate exploration on the mid Chilean coast: A geochemical and geophysical survey. *J. Pet. Sci. Eng.* **2007**, *56*, 32–41. [CrossRef]
51. Marín-Moreno, H.; Giustiniani, M.; Tinivella, U.; Piñero, E. The challenges of quantifying the carbon stored in Arctic marine gas hydrate. *Mar. Pet. Geol.* **2016**, *71*, 76–82. [CrossRef]

52. Thatcher, K.E.; Westbrook, G.K.; Sarkar, S.; Minshull, T.A. Methane release from warming-induced hydrate dissociation in the West Svalbard continental margin: Timing, rates, and geological controls. *J. Geophys. Res. Solid Earth* **2013**, *118*, 22–38. [CrossRef]
53. Ruppel, C.D.; Kessler, J.D. The interaction of climate change and methane hydrates. *Rev. Geophys.* **2017**, *55*, 126–168. [CrossRef]
54. Contreras-Reyes, E.; Völker, D.; Bialas, J.; Moscoso, E.; Grevemeyer, I. Reloca Slide: An ~24 km^3 submarine mass-wasting event in response to over-steepening and failure of the central Chilean continental slope. *Terra Nova* **2016**, *28*, 257–264. [CrossRef]
55. Geersen, J.; Völker, D.; Behrmann, J.H.; Reichert, C.; Krastel, S. Pleistocene giant slope failures offshore Arauco peninsula, southern Chile. *J. Geol. Soc.* **2011**, *168*, 1237–1248. [CrossRef]
56. Völker, D.; Geersen, J.; Behrmann, J.H.; Weinrebe, W.R. Submarine mass wasting off Southern Central Chile: Distribution and possible mechanisms of slope failure at an active continental margin. In *Submarine Mass Movements and their Consequences. Advances in Natural and Technological Hazards Research*; Yamada, Y., Kawamura, K., Ikehara, K., Ogawa, Y., Urgeles, R., Mosher, D., Chaytor, J., Strasser, M., et al., Eds.; Springer: Dordrecht, The Netherlands, 2012; pp. 379–389.
57. Geersen, J.; Völker, D.; Behrmann, J.H.; Kläschen, D.; Weinrebe, W.; Krastel, S.; Reichert, C. Seismic rupture during the 1960 Great Chile and the 2010 Maule earthquakes limited by a giant Pleistocene submarine slope failure. *Terra Nova* **2013**, *25*, 472–477. [CrossRef]
58. Klaucke, I.; Weinrebe, W.; Linke, P.; Kläschen, D.; Bialas, J. Sidescan sonar imagery of widespread fossil and active cold seeps along the central Chilean continental margin. *Geo-Mar. Lett.* **2012**, *32*, 489–499. [CrossRef]
59. USGS Science for a Changing World. Available online: https://earthquake.usgs.gov/earthquakes/ (accessed on 29 April 2019).
60. Sawyer, D.E.; DeVore, J.R. Elevated shear strength of sediments on active margins: Evidence for seismic strengthening. *Geophys. Res. Lett.* **2015**, *42*, 10–216. [CrossRef]
61. Brothers, D.S.; Andrews, B.D.; Walton, M.A.; Greene, H.G.; Barrie, J.V.; Miller, N.C.; Brink, U.T.; East, A.E.; Haeussler, P.J.; Kluesner, J.W.; et al. Slope failure and mass transport processes along the Queen Charlotte Fault, southeastern Alaska. In *Subaqueous Mass Movements*; Lintern, D.G., Mosher, D.C., Moscardelli, L.G., Bobrowsky, P.T., Campbell, C., Chaytor, J.D., Clague, J.J., Georgiopoulou, A., Lajeunesse, P., Normandeau, A., Eds.; Geological Society: London, UK, 2018; p. SP477-30.
62. Greene, H.G.; Barrie, J.V.; Brothers, D.S.; Conrad, J.E.; Conway, K.; East, A.E.; Enkin, R.; Maier, K.L.; Nishenko, S.P.; Walton, M.A.; et al. Slope failure and mass transport processes along the Queen Charlotte Fault Zone, western British Columbia. In *Subaqueous Mass Movements*; Lintern, D.G., Mosher, D.C., Moscardelli, L.G., Bobrowsky, P.T., Campbell, C., Chaytor, J.D., Clague, J.J., Georgiopoulou, A., Lajeunesse, P., Normandeau, A., Eds.; Geological Society: London, UK, 2018; p. SP477-30.
63. Sawyer, D.E.; Reece, R.S.; Gulick, S.P.; Lenz, B.L. Submarine landslide and tsunami hazards offshore southern Alaska: Seismic strengthening versus rapid sedimentation. *Geophys. Res. Lett.* **2017**, *44*, 8435–8442. [CrossRef]
64. Giustiniani, M.; Tinivella, U.; Jakobsson, M.; Rebesco, M. Arctic Ocean gas hydrate stability in a changing climate. *J. Geol. Res.* **2013**, *2013*, 783969. [CrossRef]
65. Gorman, A.R.; Senger, K. Defining the updip extent of the gas hydrate stability zone on continental margins with low geothermal gradients. *J. Geophys. Res. Solid Earth* **2010**, *115*, B07105. [CrossRef]

© 2019 by the authors. Licensee MDPI, Basel, Switzerland. This article is an open access article distributed under the terms and conditions of the Creative Commons Attribution (CC BY) license (http://creativecommons.org/licenses/by/4.0/).

Reproduced with permission of copyright owner. Further reproduction prohibited without permission.